SOILS AND FOUNDATIONS Vol. 51, No. 2, 321–331, Apr. 2011
Japanese Geotechnical Society

A CASE STUDY ON THE IN-SITU MATRIX SUCTION MONITORING AND UNDISTURBED-SAMPLE LABORATORY TEST FOR THE UNSATURATED COLLUVIUM SLOPE

CHING-JIANG JENG[i] and TAI-AN LIN[ii]

ABSTRACT

Huafan University is located on the slope of the Ta-Lun Mountain area. The slope surface in this area is a colluvium soil cover layer with loose non-uniform particles, with high permeability. Because it is situated above a rapidly changing water table, the pore water pressure varies dynamically, depending on the weather conditions. In the dry season, most of the topsoil behaves in the unsaturated condition such that the matrix suction in the soil increases its shearing strength. In contrast, when heavy rainfall occurs, the seepage by precipitation tends to destroy the existing matrix suction. This reduction in soil strength frequently results in slope failure. This study, focuses on the variation of matrix suction of the colluvium soil in different precipitation conditions with varying vegetation at the campus of Huafan University. The analysis of the in-situ monitoring results and the laboratory test results for the undisturbed specimens taken from the field, with shearing strength and matrix suction taken into account. It is expected the results to be a useful reference for disaster protection on slopes.

Key words: colluvium slope, matrix suction, shear strength, unsaturated soil (**IGC**: A1/B3/D6)

INTRODUCTION

While extensive research has been done on the variation of stress state and shearing strength, and the influence of the soil-water characteristic curve by the likes of Fredlund and Xing (1944), Fredlund and Morgenstern (1977), Ho and Fredlund (1982), Fredlund and Rahardjo (1993), Chen (1993) and Jian (2005) et al., very little of it has been focused on colluvium soil.

Huafan University is located in northeastern Taiwan on a slope at an elevation of 500 to 550 meters with the global coordinates of E-121°41′33.6″ and N-24° 58′49.6″. In this subtropical climate, although the rainy season is between April and May, heavy rainfall is also common in summer time between July to October, and is often associated with the typhoons. The average annual rainfall in the area varies from about 2000 to 4800 mm. The surface of the slope consists of a colluvium soil, with a high permeability located close to the ground water table. Field investigations have shown that sliding surfaces are not restricted to under the saturated zone but also appear above the ground water level (Jeng, 2003).

Heavy rainfall frequently induces slope instability problems (Jeng et al., 2007; Jeng and Su, 2008). The water content and matrix suction of unsaturated soil are strongly dependent on the weather conditions. When it rains heavily, the matrix suction, located primarily in the unsaturated soil, is more or less destroyed, forming a wet zone, and reducing the effective strength of the soil. This sometimes leads to the sliding of the slope (Gasmo et al., 1999). A thorough understanding of the sliding problem of unsaturated colluvium slope requires variations in soil water content and matrix suction to be monitored (Tsao and Chang, 2007; Kung and Lin, 2005).

To help ensure the safety of the buildings on the campus and for the purposes of contributing to efforts to monitor potential landslides, an integrated monitoring system including 29 holes of inclinometers, tiltmeters, surface extensometers, crack gauges, observation wells and hundreds of settlement and displacement observation marks were set up across the campus. Data was collected continuously over the seven years since the monitoring system was put into practice. The results of the inclinometers (Jeng, 2003; Jeng et al., 2007) showed that the deformation mechanism of the slope corresponds to the thickness distribution of the top colluvium layer, the rainfall, construction and earthquake factors. Among these factors, the rainfall associated with typhoons is the most significant. Jeng and Su (2008) collected all the settlement and displacement data observed from the observation marks induced by natural hazards. The data revealed three increments of settlement and displacement that coincided with threshold levels of rainfall and seismic activity.

[i] Associate Professor, Department of Environmental and Hazards-Resistant Design, Huafan University, Taiwan (jcjhf@cc.hfu.edu.tw).
[ii] Master, ditto.
The manuscript for this paper was received for review on June 17, 2009; approved on February 7, 2011.
Written discussions on this paper should be submitted before November 1, 2011 to the Japanese Geotechnical Society, 4-38-2, Sengoku, Bunkyo-ku, Tokyo 112-0011, Japan. Upon request the closing date may be extended one month.

On-going research involving the monitoring of variations in the soil suction of the colluvium is being carried out. In this study, we report on the results of additional new inspection instruments, including devices to measure the matrix suction, water content and ground water level, all of which were set up during different surface planting conditions. The matrix suction and water content data for each depth in real-time were collected, and the laboratory tests for the undisturbed specimens taken from the field were analyzed. The relationships of shearing strength and matrix suction for the colluvinm soil were determined. These results can serve as a reference for the study of slope stability mechanisms.

Topography and Geology and Natural Environment of the Slope

The elevation of the sloping surface varies from 500 to 550 meters (i.e., a little higher than the top of the skyscraper Taipei 101). Figure 1 shows the topography plan of the slope and Figs. 2 to 5 illustrate the geological profiles of sections A to D. From a geological point of view, the university is constructed on a dip slope.

The monitored slope is characterized by variations in the soil suction (hereafter called the target slope). Figure 6 shows the detail soil profile of the target slope. It comprises an overburden of colluvium with a nonuniform particle size distribution, sitting atop Miocene sandstones and shales, above bedrock. The unified soil classification of this overburden is between GW and SW. The maximum particle size is between 152.4 mm to 63.5 mm (Jeng et al., 2005). The seepage properties of the top soil were determined by the Guelph permeameter. The hydraulic conductivity value of the short grass zone, the long grass zone and the broadleaf tree zone are 0.000286, 0.00023 and 0.000129 cm/sec, respectively. The average value is 0.000215 cm/sec. The annual mean temperature and maximum precipitation exceed 20°C and 5,227 mm, respectively (Fu, 2004). The monsoon, from the northeast, usually results in overcast and rainy weather in the winter. The daily temperature variation in the winter is not significant, while changes of more than 5°C are typical between day and night in the summer time. Typhoon-induced heavy rainfall occurs in summer due to the effects of the warm, wet current from the southwest.

The target slope has an average gradient of about 30 degrees, sloping more gently to 15 degrees at the top and foot. Three different surface planting areas have been classified in this study: (1) a short grass zone at the top area, (2) a broadleaf tree zone in the middle, and (3) a 70 centimeter grassy zone at the foot of the slope. Figure 6 shows the geologic strata profile and the three distinct

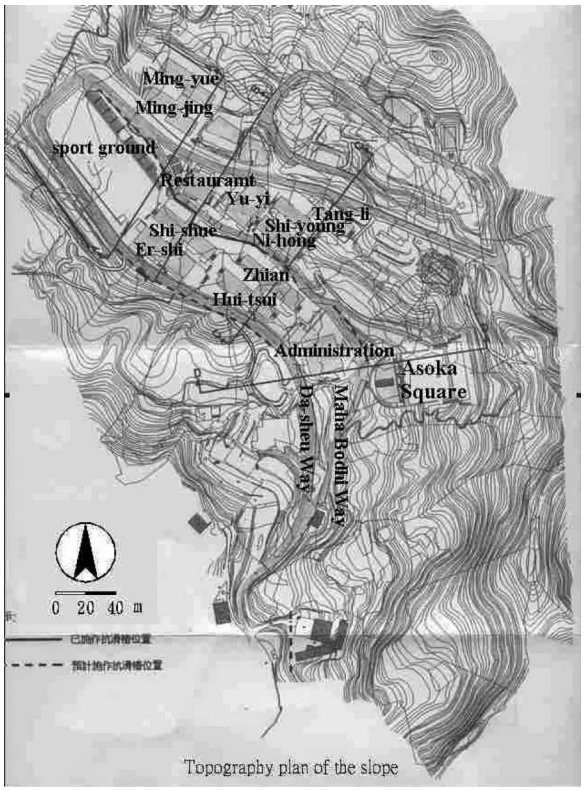

Fig. 1. Topography plan of the slope

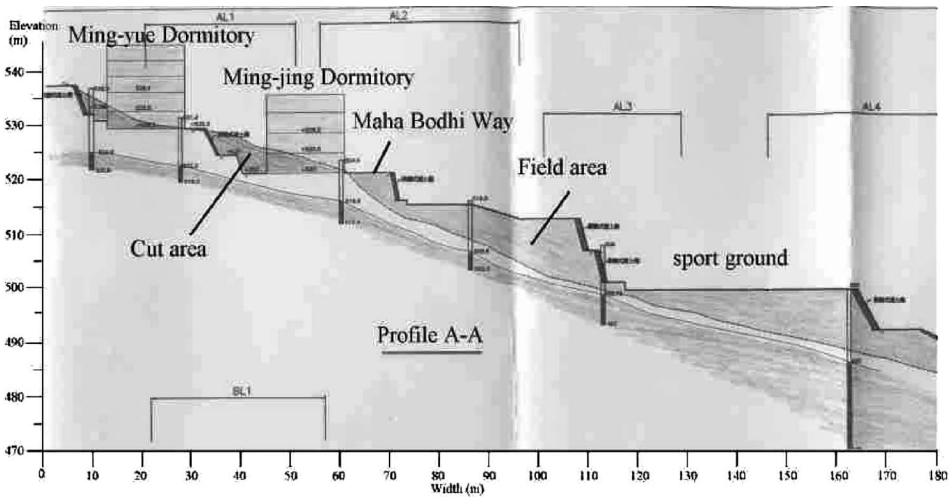

Fig. 2. Profile A-A

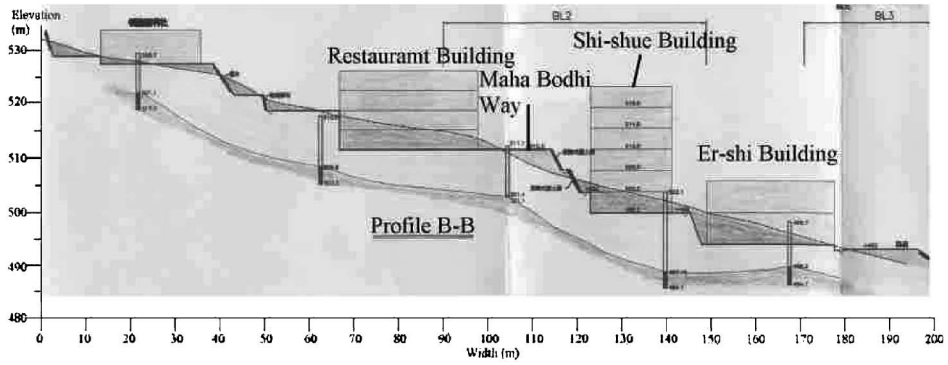

Fig. 3. Profile B-B

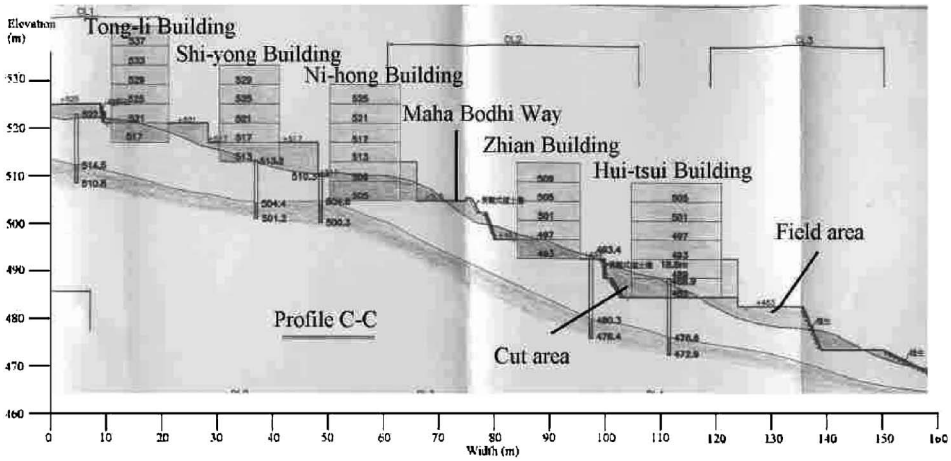

Fig. 4. Profile C-C

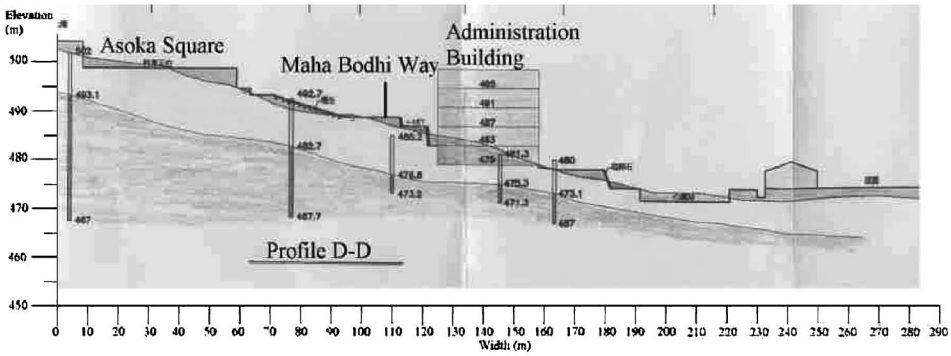

Fig. 5. Profile D-D

surface planting zones.

Field Monitoring Plan

A monitoring plan for the target slope, including the measurements of the field matrix suction and water content variations of the three different planting zones, was put into place. Ten sets of electrical tensilmeters, four sets of soil moisture meters, and one set of water level meters were embedded in three boreholes located in each planting zone. Two tensilmeters were set in the short grass zone, one each at two and four meters depth, four sets placed in the broadleaf tree zone at 2, 3, 4 and 5 meters in depth, respectively, while four more sets were embedded in the long grass zone at 2, 4, 6 and 8 meters in depth, respectively. Four soil moisture meters were separately installed in each of the boreholes at a depth of 2 meters, and additionally one was installed at 8 meters in depth in the long grass zone.

The installed measuring devices were numbered in sequence from the top of the slope to the foot, as shown in Fig. 7. Table 1 shows the detailed installed elevation of all the measuring devices. The soil matrix suction and

water content measured in the field were then correlated with the precipitation records obtained on campus. The analysis of the data allowed the phenomenon of reduction in soil matrix suction caused by rainfall to be observed. The reduction in soil strength is expected to conitnue progressively and lead to slope failure occurs.

MONITORING RESULTS AND ANALYSIS

Potential Surface Failure and Ground Water Condition

Figure 8 shows the profile of the potential surface failure and ground water table of the monitoring slope. The potential surface failure in Fig. 8 is obtained from the monitoring results of the adjacent inclinometer (Jeng and Hsieh, 2010). According to the results obtained from the two observation wells, the potential surface failure may pass through above the existing ground water table. As such, it may be that the surface failure of the slope may originate in the unsaturated soil layer.

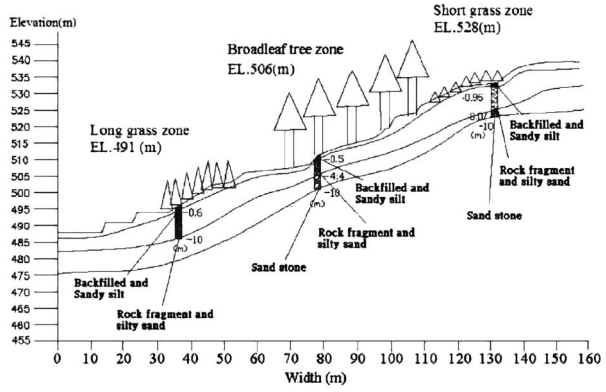

Fig. 6. Stratigraphy profile of the target slope

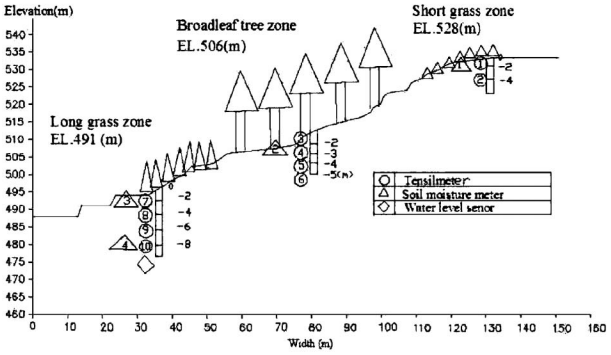

Fig. 7. Location of monitoring devices in the target slope

Relationship between Matrix Suction and Precipitation

Data recorded during the continuous monitoring of the slope from March 2, 2005 to September 21, 2005, was examined in this study. During this monitoring period, a lacunae in the data occurred when lightning destroyed the data recorder. Figure 9 shows the precipitation records during this period. For convenience, this period will be further divided into three time segments: March to April, when the weather is usually cloudy and wet due to frequent rain of low intensity (less than 10 mm/hr); May to June, when continuous rain, due to thunderstorms, exceeds 20 mm/hr; and July to September, when average temperatures are the highest for the year, and rain is seldom continuous, but typhoons visit the island (four during the period under discussion).

Figures 10 through 12 show the matrix suction and precipitation data for the three periods. Results from the

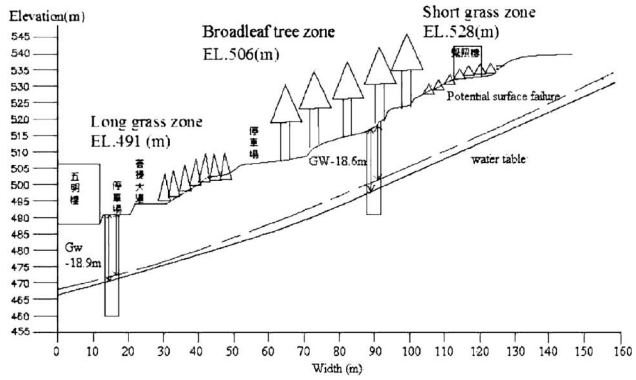

Fig. 8. Profile of potential surface failure and ground water table

Table 1. Elevation of all the measuring devices

Short grass zone (Surface EL. 528 m)						
Apparatus	T-1	T-2	M-1			
EL. (m)	526	524	526			
Broadleaf tree zone (Surface EL. 506 m)						
Apparatus	T-3	T-4	T-5	T-6	M-2	
EL. (m)	504	503	502	501	504	
Long grass zone (Surface EL. 491 m)						
Apparatus	T-7	T-8	T-9	T-10	M-3	M-4	W-1
EL. (m)	489	487	485	483	489	483	481

Note: T-1 denote No. of tensimeter; M-1 denote No. of soil moisture meter; W-1 denote No. of water level meter; EL. denote elevation.

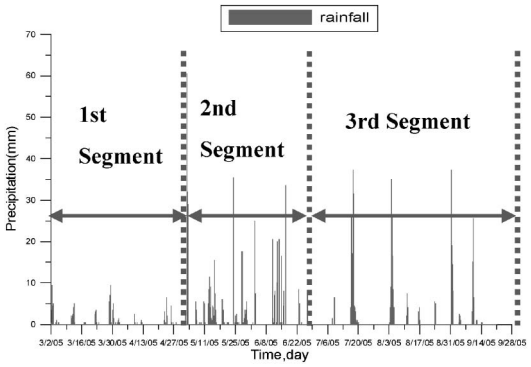

Fig. 9. Precipitation record of project site

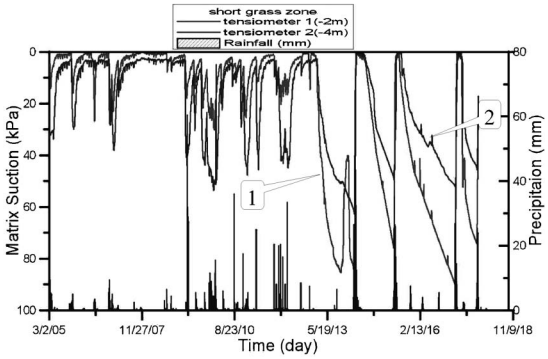

Fig. 10. Relationship between matrix suction and precipitation in short grass zone

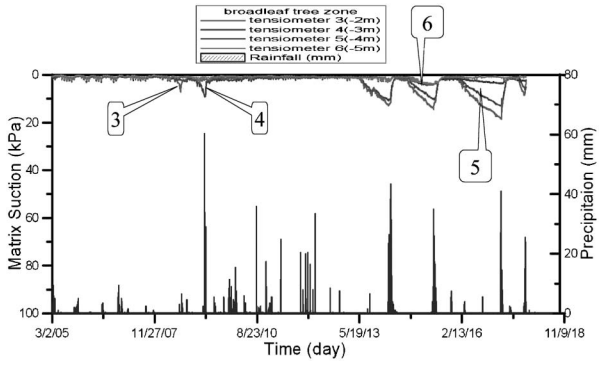

Fig. 11. Relationship between matrix suction and precipitation in broadleaf tree zone

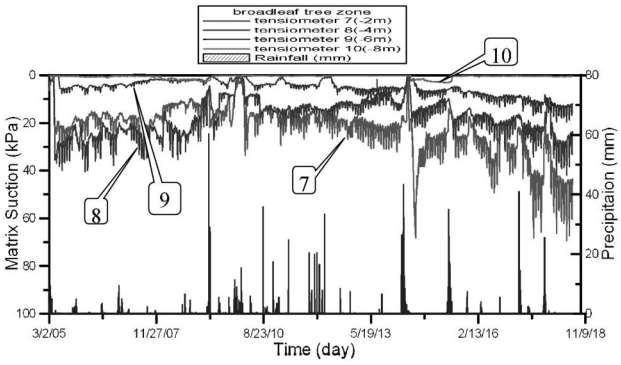

Fig. 12. Relationship between matrix suction and precipitation in long grass zone

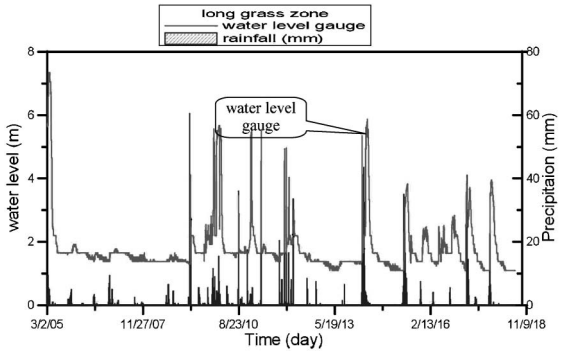

Fig. 13. Relationship between ground water level and precipitation in long grass zone

figures indicate that for the short grass zone, regardless of the time period, a higher suction occurs than in the other planting zones. In the third time segment (i.e., July to September) shown in Fig. 10, the cumulative maximum suction value in the short grass zone at two meters depth (No. 1 in Fig. 10) is highest at 90.3 kPa. In the second time segment (i.e., March to June), the maximum suction value in the short grass zone appears at four meters depth (No. 2 in Fig. 10), at 43.8 kPa. Although the short grass zone possesses the highest suction value in summer, the matrix suction in the short grass zone is destroyed during strong rain, such as that falls during a typhoon. The larger the variation in the matrix suction caused by rainfall in the short grass zone, the lower the slope protection from failure.

The broadleaf tree zone shown in Fig. 11 has lower levels of suction and preserves water the best. During rainfall, a portion of the falling water is intercepted by the canopy, some of it passing through to the ground surface of the forest. When the intensity of precipitation is great, most of the water reaches the ground surface and either seeps into the soil or is stored within voids in the soil (Chen, 1993). Figure 11 shows that the suction value in the broadleaf tree zone is the lowest, while the frequency of variation is the greatest. This can be attributed to the forest cover, which causes most of the runoff to be retained before it seeps into the soil. Moreover, because of the tree roots, there is an increase in the number of voids in the soil, which improves the infiltration of the water.

The long grass zone in the toe of the slope absorbs runoff water from the upper hill and therefore can easily raise the ground water table. Figure 13 shows the relationship between the ground water level and the precipitation in the long grass zone at a depth of 10 meters. Based on the results shown in the curve, the normal water level is about GL-8.4 m. It quickly approaches the depth of the No. 10 tensilmeter. Thus, the value of the No. 10. curve in Fig. 12 is consistently at zero. The runoff and seepage water from the upper hill no doubt has an

effect on the suction value of other depths in the long grass zone.

A comparison of the shallow layers (2 m and 3 m) and deeper layers (lower than 4m) is shown in Figs. 10 to 12. In the first and second time segments, the suction value in the shallow layers is larger than in the deeper layers.

Time Lag in Suction Response to Rainfall

At the commencement of precipitation, the rainfall falling from the sky to the ground passes through the canopy and is held by the plants. This lengthens the time required for a change in suction, leading to a time lag in the suction change response. Figures 14 to 16 indicate precipitation began at 17:00 hours on March 29, 2005 and again at 16:00 hours on March 30, 2005, with an interval of about 10 hours between these events. The maximum intensity was 9.5 mm/hr and 4 mm/hr with durations of 25 hours and 12 hours, respectively. The time lag of suction response in the three zones for the depth of 2 meters was analyzed. The time lag in the suction change response for the short grass zone in Fig. 14 is 13 hours and 18 hours, respectively. Figures 15 and 16 show that the first precipitation had no effect on the suction response in the long grass and broadleaf zones. No reduction in suction was observed until the second rainfall commenced, leading to a time lag of 72 hours and 84 hours for each case. Time lag in the broadleaf tree zone (i.e., Fig. 16) was the longest. From the view point of time lag in suction response, the forest cover area (i.e., broadleaf tree zone in Fig. 16) is the most effective at ameliorating the effects of rainfall. Thus, the broadleaf zone protects the slope better than other plant cover. This conclusion is made only from the view point of the time lag effect. Because of this time lag effect, rainfall over short durations may have no influence on the broadleaf tree zone, although the short grass zone undergoes a decrease in matrix suction. With regard to small suction value measured from the broadleaf tree zone, the shear strength obtained from the reinforcement effect of the roots probably is likely to be higher than the loss in the small suction value. However, more research is required to confirm this, and it is not the focus of this paper.

Undisturbed Specimens Laboratory Test

In addition to the in-situ monitoring results, triaxial compression tests and pressure plate matrix suction measurements were carried out in the laboratory. Large-sized specimens of undisturbed soil samples were collected from the target slopes of Huafan University campus, with dimension of 18 inches in height and 9 inches in diameter. In order to obtain the shear strength parameters, like cohesion and the friction angle, both saturated and unsaturated unconsolidated undrained triaxial test were done. The relationship between shearing strength and matrix suction was determined from the results of the triaxial compression test. The soil-water retention curve was then derived from the pressure plate matrix suction measurement to obtain the relationship between water content and matrix suction. The data obtained from the in-situ and laboratory work stands to serve as a valuable reference for landslide mitigation.

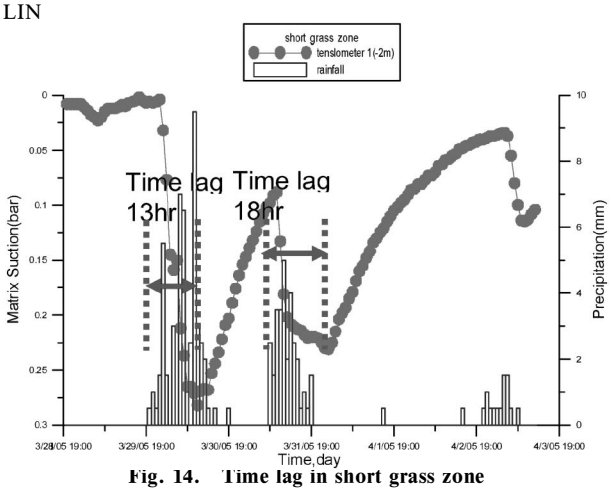

Fig. 14. Time lag in short grass zone

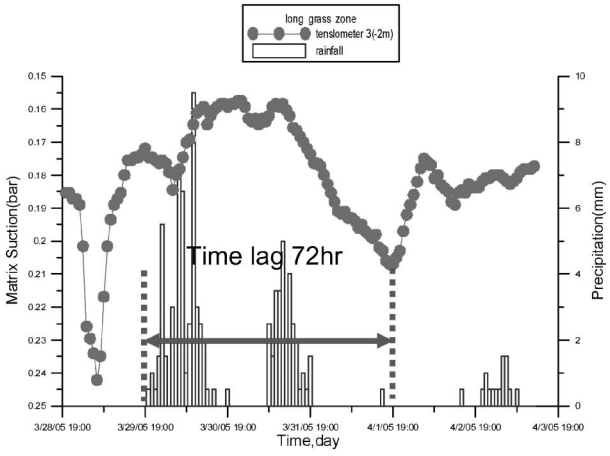

Fig. 15. Time lag in long grass zone

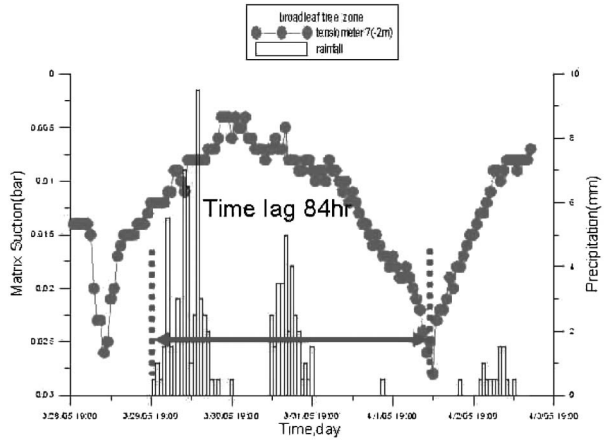

Fig. 16. Time lag in broadleaf tree zone

Process and Results of Saturated Triaxial Test

Due to the rare large-size specimens, a multiple stage triaxial test was conducted with re-rising σ_3 to the specimen after pre-stage testing was accomplished. Four chamber-confining pressures σ_3 were selected: 50, 100,

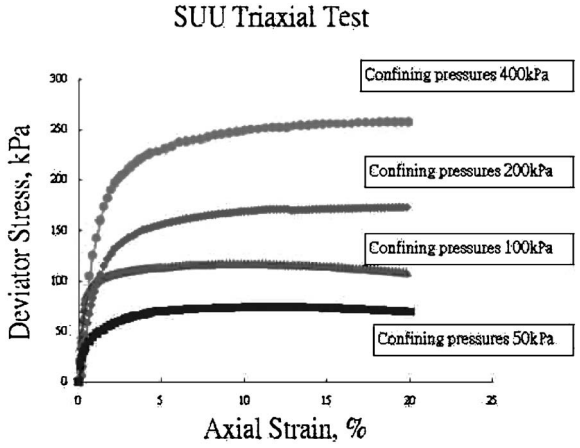

Fig. 17. Stress-strain relation curves of SUU triaxial test

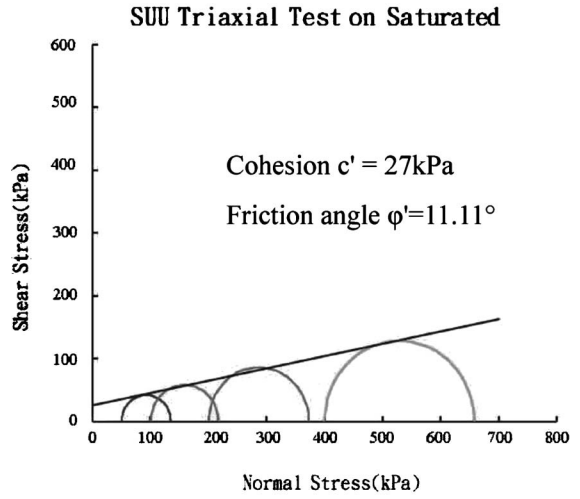

Fig. 18. Failure envelope of SUU triaxial test

200 and 400 kPa. The corresponding deviator stresses were 85, 117, 173 and 258 kPa, respectively. The stress-strain curves are shown in Fig. 17. The shear strength parameters C′ was 27 kPa and φ' was 11.11 degrees. They were determined by plotting Mohr's circle at failure, as shown in Fig. 18.

Process and Results of Unsaturated Triaxial Test

In this case, the triaxial test equipment and process for preparing samples are identical to the above-mentioned saturated unconsolidated undrained triaxial test. The only differences between the unsaturated and saturated triaxial tests are that a constant-head water pressure of 2 m in height was applied to the unsaturated specimen in the process of saturation. The net confining pressure was kept constant, at 100 kPa. For the sake of determining the relationships between the shearing strength and matrix suction, specimens were subjected to distinct matrix suctions of 10, 30, 50, 100, 200 and 400 kPa, respectively. The matrix suctions were achieved by turning up the cell pressure and air pressure simultaneously, and by keeping the water pressure constant. The confining

Table 2. Results of total cohesion and friction angle corresponding to various matrix suction

Matrix suction (u_a-u_w), (kPa)	Total cohesion C, (kPa)	φ' degree	φ_b degree
(a) 0.0	27	11.11	0
(b) 10	37	11.11	45
(c) 30	48	11.11	34.9
(d) 50	58	11.11	31.8
(e) 100	66	11.11	21.06
(f) 200	71	11.11	12.41
(g) 400	76	11.11	6.98

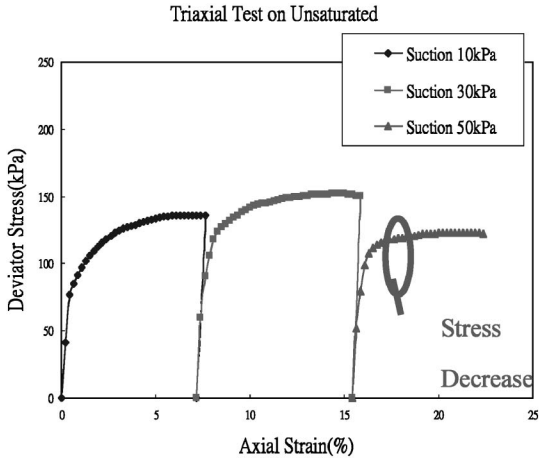

Fig. 19. Stress-strain relation curves for various matrix suction

pressure is equal to the cell pressure minus the air pressure. The matrix suction is equal to the air pressure minus the back water pressure. The axial load applied by the loading ram corresponding to the axial deformation was measured by a load cell. When axial loading tests were completed, the specimens were left in the triaxial chamber. When the axial load was relieved, the matrix suction increased and the next stage of the triaxial compression test was conducted. In order to minimize the effects of multiple tests on the same specimen (e.g., shearing the specimen), no more than three tests were performed on any one specimen. Among the three test results, the one which deviated from the others was ignored.

The strength parameters are shown in Table 2. Figures 19 though 22 show the stress-strain responses of unsaturated triaxial tests. According to Figs. 19 and 20, and Table 2, the deviator stress and cohesion increased as the matrix suction increased. However, the deviator stress only slightly increases while the matrix suction is equal to or more than 200 kPa. This is also seen in Fig. 23, which summarizes the results of the saturated and unsaturated triaxial test (extended 3-D shear strength failure envelope). The failure envelope for the saturated condition shown in Fig. 18 is with a matrix suction of zero (i.e., line (a) in Fig. 23). The friction angle φ_b, derived from matrix

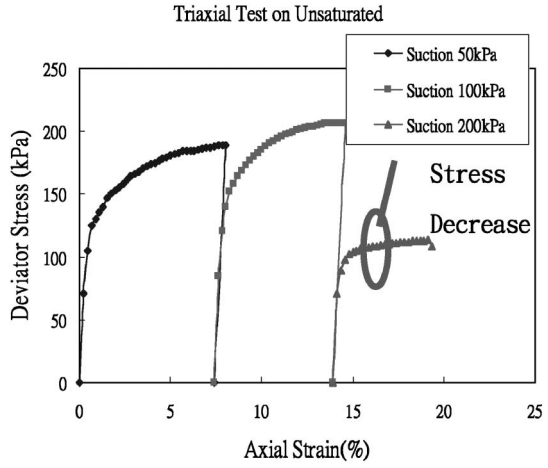

Fig. 20. Stress-strain relation curves for various matrix suction

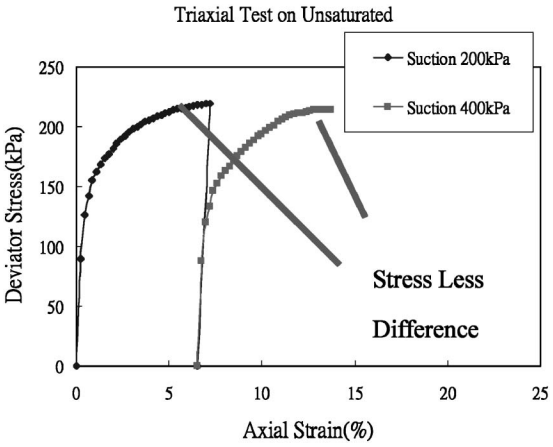

Fig. 21. Stress-strain relation curves for various matrix suction

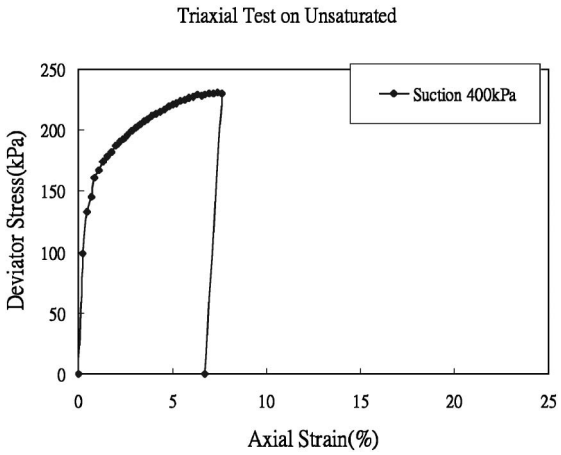

Fig. 22. Stress-strain relation curves for various matrix suction

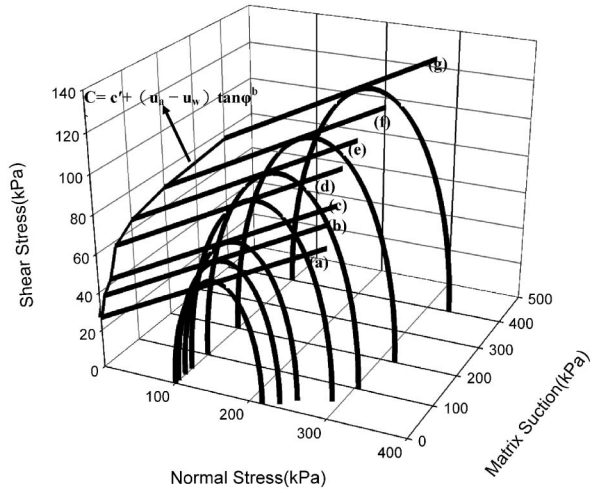

Fig. 23. Extended 3-D shear strength failure envelope

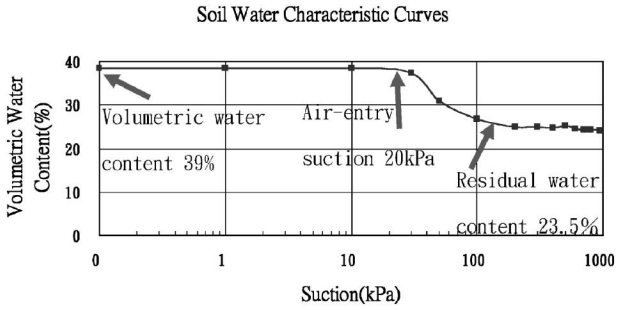

Fig. 24. SWRC from the laboratory pressure plate measurement

suction decreases with increasing matrix suction. Thus, shear strength increases only slightly when matrix suction is greater than 200 kPa. According to Figs. 19 and 20, the deviator stresses decreased on the last testing curve, so that data was disregarded. The decrease in shear strength when matrix suction was greater than 200 kPa may be due to the effect of the residual suction (ψ_r) corresponding to the residual water content (θ_r). The curve of SWRC shown in Fig. 24 shows the residual suction to be about 200 kPa. Escario and Juca (1989) suggested that the soil-water-air interphase relationships have a large influence on the engineering behavior of unsaturated soils. As the soils move from a saturated condition to a dry condition, the shear strength increases non-linearly and may even start to decrease at large values of suction for unsaturated soils. Chu (2004) came to the same conclusion in his investigation on Linkou Terrace Unsaturated Lateritic Soil.

Comparison of the Soil-water Retention Curve Derived from the Pressure Plate Measurement and In-situ Monitoring Results

The Soil-water Retention Curve (SWRC) is the relationship between matrix suction and the degree of saturation (or volume water content) reflecting soil strength, seepage and the constitutive structure. In addition, during the process of drainage and absorption, the matrix suction is related to different degrees of saturation (or volume water content). This implies that the drainage path is different from the absorption path. For this reason, understanding the variations in the SWRC, which

can be attributed to a number of factors, is the key to understanding the water retention in soil.

The drying process of the SWRC (i.e., drainage curve) from pressure plate measurements has been successfully derived, as shown in Fig. 24. Undisturbed soil samples for pressure plate tests were collected from campus slopes with a dimension of 4 in. in diameter and 1 in. in height. Water was sprayed on the specimen until moisture was exuded. Then, the specimen was put in the pressure plate with an air pressure of 1, 10, 30, 50, 100, 200, 300, 400, 500, 600, 700, 800 and 950 kPa, respectively. Each air pressure was sustained for 24 hours to reach suction equilibrium and the corresponding moisture weights were measured. Finally, the specimen was taken out and put in the oven to be dried. With the dry weight of the sample, the relationship between the suction and volume water content was determined.

According to Fig. 24, the initial stage volume water content was 39% in the condition of saturated soil and the residual volume water content was about 23.5%. The variation in the water content from the saturated to residual condition was therefore about 15.5%. In contrast, no effect on the volume water content was observed when the suction was less than 20 kPa. Nevertheless, when the suction was more than 20 kPa, the water in the soil experienced significant drain off. The moisture ceased to drain when the suction reached 200 kPa. It can be concuded that the air entry value of in situ soil is about 20 kPa.

Figures 25 through 27 show the in-situ SWRC of the shallow soil (2 m depth) for different planting zones in the time segments of July to September when the change and divergence of dry and humid days was apparent. In view of those curves, it was found that although it is difficult to obtain the wetting process of the SWRC (i.e., absorption curve) in the laboratory by the pressure plate measurement, the drying and wetting process of the soil was implied in the in-situ SWRC results, as shown in Figs. 25 to 27. The behavior of hysteresis was included as well. Nevertheless, the in-situ SWRC does not fully agree with the results from the laboratory tests because the action of wetting and evaporation occurs simultaneously in the natural environment, while in the laboratory tests, only one condition was applied at a time. During the rain, before the moisture in the soil approaches the air entry value, drainage has already commenced. The in-situ matrix suction differs from the laboratory pressure plate condition by more than 100 kPa, as shown in Fig. 24. However, the variation of volume water content in the field was in the same range as that in the laboratory (i.e., from 39% to 23.5%).

For comparative purposes, the largest matrix suction and the most scattered data points are displayed in the short grass zone (Fig. 25). The short grass zone has the highest matrix suction, at 90.3 kPa, in the third time segment. This is due to the higher temperatures and longer periods of sunlight in this time segment. The hysteresis effect is apparent here. The smallest matrix suction and the most concentrated data points are displayed in the

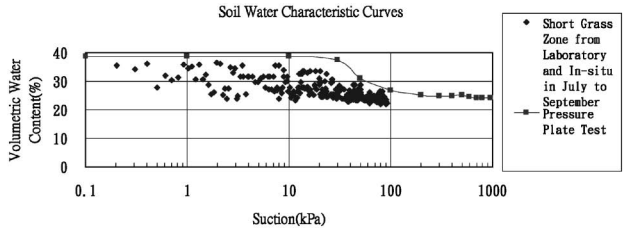

Fig. 25. SWRC for short grass zone from laboratory and in-situ in July to September

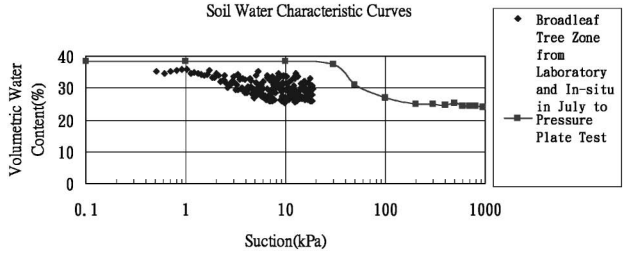

Fig. 26. SWRC for broadleaf tree zone from laboratory and in-situ in July to September

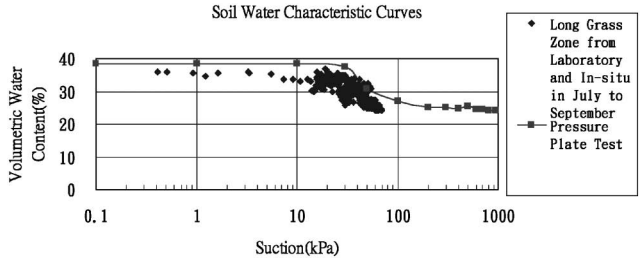

Fig. 27. SWRC for long grass zone from laboratory and in-situ in July to September

broadleaf tree zone (refer to Fig. 26). This demonstrates that the forested area retains more water, and the difference in water content between the wet season and hot season is the least significant. It indicates that moisture in the soil moves quickly and small water circuits can form. The water often starts to move from wet to dry in circles when the suction reaches 20 kpa, a number supported by the air entry value obtained from the pressure plate measurement. The SWRC of the long grass zone (Fig. 27) is similar to the pressure plate measurements. The air entry value is about 15 kpa, but no hysteresis effect is evident.

The SWRC of the drying curve derived from the pressure plate measurements (shown in Fig. 24) is different from the in-situ condition (the diamond point shown in Figs. 25–27). This is not due only to the plant type but to the interactive exchange of drying and wetting states which occur in the field. Huang et al. (2004) point out that changes in the water content of unsaturated soil occur due to a series of complicated hydrological processes, including infiltration, evaporation and evapotranspiration. The dynamic change of soil water content generally does not follow the same path as the soil water retention

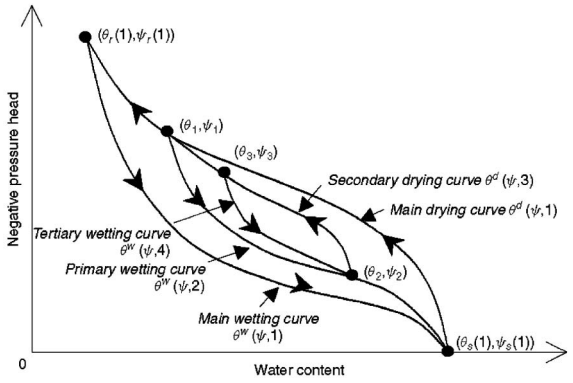

Fig. 28. SWRC for theoretical model of in-situ states (Huang et al., 2004)

curves. Besides the main drying and main wetting curves, there are primary drying curves, primary wetting curves and a series of scanning curves, as shown in Fig. 28.

CONCLUSIONS

After an extensive literature review on the matrix suction of unsaturated soil, it was found that only a few studies have been done on colluvium soil. This may be because the integrated field observation for corroboration is difficult to obtain. The in-situ observation results of matrix suction and the the SWRC from laboratory pressure plate measurements were discussed, and the shearing strength was considered in terms of the matrix suction. Based on the analyses from lab and field test results, several conclusions were made.

The suction of the short grass zone, regardless of the time period, is higher than in the other planting zones. The cumulative maximum suction value in the short grass zone at two meters depth is the highest at 90.3 kPa. The suction value in the broadleaf tree zone is the lowest, which can be attributed to the improved infiltration of the water provided by the forest cover and the voids in the soil around the tree roots. The difference in water content between the three zones is more evident in the third time segment. However, besides the plants conditions, there may be other minor factors such as the position and surface slope of the three zones that make it difficult to distingush betweeen the vaious factors.

According to the monitoring results, no matter what planting zone, the change of matrix suction caused by rainfall is more apparent in the shallow layer than in the deeper layer. The change in the value of matrix suction in the shallow layer is more obvious than in the deeper soil. When a light rain falls in a short time period, the matrix suction in the deeper layer remains the same.

In the case of the third time segment, because the higher mean temperature and the effect of evaporation caused by sunlight are stronger, the matrix suction in this time segment is higher. However, when heavy rains caused by typhoons fall on the area, matrix suction drops quickly. This variation is obvious in the short grass zone and less clear in the broadleaf tree zone. The maximum value in the short grass zone, long grass zone and broadleaf tree zone at 2 m depth are 90.3 kPa, 68.2 kPa and 18.5 kPa, respectively.

The time lag in suction change for the short grass zone is 13 hours and 18 hours, respectively. In the long grass and broadleaf tree zones, there is a time lag of 72 hours and 84 hours for both. This implies that the broadleaf zone protects the slope better than other plant cover. This conclusion is made only from the view point of the time lag effect. Because of this time lag effect, short periods of rainfall may have no influence on the broadleaf tree zone, although the short grass zone experiences a decrease in matrix suction almost immediately. With regard to the other view point of small suction value measured from the broadleaf tree zone, the shear strength obtained from the reinforcement effect obtained from the roots probably could be higher than the accompanying loss in the suction value. However, this particular issue requires further investigation and is not within the scope of this paper.

In this study, an extended 3-D shear strength failure envelope was created. The friction angle ϕ_b, derived from the matrix suction decreases when the matrix suction is greater than 200 kPa.

Based on the pressure plate measurements, the initial water volume content is 39% for saturated soil and the residual water volume is about 23.5%, indicating a variation of 15.5% between the two conditions. The air entry value of in-situ soil is about 20 kPa.

The disagreement between the in-situ SWRC and the laboratory test results is because under the natural environment, the action of wetting and evaporation occur simultaneously, while in the laboratory test only one condition was applied at a time. However, the variation of water content in the field was in the same range in both the laboratory and in the field.

The SWRC of the long grass zone is very similar to the result of the pressure plate measurement. The air entry value is about 15 kpa, but no hysteresis effect was evident.

REFERENCES

1) Chen, M.-C. (1993): Research on the characteristics of soil void distribution in different forest area of Lian-fua pool, *Quarterly Jounal of Chinese Forestry*, **26**(2), 63–77.
2) Chu, H. A. (2004): Engineering properties of Linkou terrace unsaturated lateritic soil, *Master thesis*, National Taipei University of Technology.
3) Escario, V. and Juca, J. (1989): Strength and deformation of partly saturated soils, *Proc. 12th International Conference on Soil Mechanics and Foundation Engineering*, Rio de Janeiro, **3**, 43–46.
4) Fredlund, D. G. and Xing, A. (1944): Equation for the soil-water characteristic curve, *Can. Geotech. J.*, **31**(4), 521–532.
5) Fredlund, D. G. and Morgenstern, N. R. (1977): Stress state variable for unsaturated soils, *Journal of Geotechnical Engineering*, ASCE, GT5, **103**, 447–446.
6) Fredlund, D. G. and Rahardjo, H. (1993): *Soil Mechanics for Unsaturated Soils*, John Wiley and Sons, New York.
7) Fu, Y.-W. (2004): Climatic analysis of Ta-lun mountain in 2004, *Master thesis*, Fuafan University.
8) Gasmo, J., Hritzuk, K. J., Rahardjo, H. and Leong, C. (1999): In-

strumentation of an unsaturated residual soil slope, ASTM, *Geotechnical Testing Journal*, 134–143.

9) Ho, D. Y. F. and Fredlund, D. G. (1982): Increase in strength due to suction for two Hong Kong Soil, *Proc. ASCE Specialty Conference on Engineering and Construction in Tropical and Residual Soil, Hawaii, 263–296*.
10) Huang, H.-C., Tan, Y.-C., Liu, C.-W. and Chen, C.-H. (2004): A novel hysteresis model in unsaturated soil, *Hydrological Processes*.
11) Jeng, C.-J. (2003): Study on slope stability mechanism of Huafan University by using of inclinometer displacement and limiting equilibrium stability analysis, *Journal of Huafan University*, (9), 115–127.
12) Jeng, C.-J., Lin, T.-A., Hsu, J.-K. and Chen, S.-H. (2005): Study on the particle size simulation of colluvium and its shearing characteristic, *Proc. 2005 Culture and Design Conference*, Fuafan University, 445–454.
13) Jeng, C.-J., Li, C.-T., Chen, S.-F. and Lue, C.-H. (2007): Case study on time dependent displacement monitoring results and their influence factors for the slope land, *Journal of Huafan Art and Design*, (3), 195–209.
14) Jeng, C.-J. and Su, D.-Z. (2008): Case study on the settlement and displacement monitoring results on a slope induced by natural hazards, *Proc. 3rd Taiwan-Japan Joint Workshop on Geotechnical Hazards from Large Earthquakes and Heavy Rainfall*, 119–130.
15) Jeng, C.-J. and Hsieh, T.-Y. (2010): A case study on the analysis of a monitored slope and the judgment to the sliding surface, *Journal of Huafan Art and Design*, (6), 1–14.
16) Jian, Z. (2005): Main influences on soil water retention curve, *Proc. the Second Chinese National Symposium on Unsaturated Soils*, Hangchow, 390–400.
17) Kung, J. and Lin, H.-T. (2005): Influence of vegetation on the slope stability of unsaturated soil slop, *Proc. 11th Conference on Current Researches in Geotechnical Engineering in Taiwan*, c17–1–c17–8.
18) Tsao, S.-P. and Chang, T.-J. (2007): Study of soil water characteristic curve on sand box experiments, *Proc. Annual Congress of Chinese Soil andWater Conservation Society*.